Journal of Sound and Vibration (2001) **248**(2), 267–288
doi:10.1006/jsvi.2001.3787, available online at http://www.idealibrary.com on IDEAL®

DYNAMIC AMPLIFICATION FACTOR AND RESPONSE SPECTRUM FOR THE EVALUATION OF VIBRATIONS OF BEAMS UNDER SUCCESSIVE MOVING LOADS

E. SAVIN

Structural Dynamics and Coupled Systems Department, ONERA, BP72, 92322 Châtillon Cedex, France. E-mail: Eric.Savin@onera.fr

(*Received* 20 *November* 2000, *and in final form* 5 *March* 2001)

Analytic expressions of the dynamic amplification factor and the characteristic response spectrum are derived for weakly damped beams with various boundary conditions subjected to point loads moving at constant speeds. These coefficients are given as functions of the ratio of the span length to the loads wavelength, and the loads wavelength respectively. They allow a rapid calculation of the vibration amplitudes induced by a succession of moving loads on a beam. These results are particularly useful in the context of railway bridges preliminary design and assessment of the expected maximum vibration levels under high-speed trains.

1. INTRODUCTION

The literature dealing with moving loads on bridges is considerable and has been enriched in the last few decades by the development of high-speed rail networks in continental Europe and Asia. A comprehensive review of these works is out of the scope of this paper, and the various references below are just given as non-exhaustive indications for further reading. Nevertheless, it appears that most of the recent studies focus on numerical simulations, possibly including the effects of train mass inertia, coupling with the train cars suspension systems, tracks stiffness, damping and roughness, especially for ballasted tracks, or rail–wheel contact (see for instance, the recent works [1–6]). Comparatively few studies concentrate on analytical developments, although the analytical solutions of a beam traversed by a single point load is well known (see references [7–11] and references therein) provided that simple assumptions are used for the description of the load, mainly neglecting its inertia effect. Fewer works deal with the possible dynamic amplifications induced by a regular succession of loads, as is the case for railway bridges when the frequency of succession matches their natural frequencies [12–15]. Note that such analytical developments can also be performed up to a thorough level for the case of a moving load on an elastic half-space, with applications to the evaluation of the characteristics of guided waves induced by trains in the trackbed, ground vibrations in the environment or possible instabilities [16, 17]. Another major subject of interest has been the consideration of some randomness in the train speed, loads spacing and/or amplitudes [11, 18, 19], track roughness [20–22] or track stiffness characteristics [23]. These latter cases are probably the most relevant ones when applied to modern railways although the most difficult to handle from a theoretical point of view; on the contrary, randomness related to the loads amplitudes, speed or arrival times, is more likely to occur for highway bridges.

0022-460X/01/470267 + 22 $35.00/0

Most studies focus on the assessment of the dynamic deflection of a beam induced by the moving loads for application to structural strength design. Practically, this point is seldom a real concern for prestressed concrete railway bridges since, firstly, they are primarily designed for heavy static loads, including the prescribed dead loads and train loads, and secondly, viscous damping is often rather important (a minimum of about 5% of critical damping). Steel or composite steel/concrete bridges have much lower damping rates (about 0·5%) but they are also usually stiff enough to withstand dynamic amplifications from train loads. The main concerns for railway engineers are in the evaluation of riding comfort when trains traverse bridges, running safety, and tracks stability and deformation. Riding comfort is basically related to the vertical and transverse accelerations experienced inside the train cars; running safety is ensured at least if a continuous contact can be kept between the wheels and the rails; rails deformation is a critical point for modern railways where continuous welded rails are used [24], whereas it is necessary to avoid any possible decohesion of the ballast whenever it is used. Therefore, vertical accelerations, rotations at abutments and supports, torsion or warping are the most relevant quantities to focus on. The usual criteria to be fulfilled for them may be found, for instance, in reference [25]. The last issue worth mentioning from an engineering point of view is the analysis of fatigue in operational conditions, namely the repetition in time of such regular loadings at very high speeds (more than 250 km/h) for each direction on the bridge. Composite bridges may be particularly sensitive to this phenomenon which needs to be carefully evaluated for the structure itself as well as its various connections [24–26]. Use of ballasted tracks and concrete decks has the advantage of significantly enhancing their behaviour [25].

The purpose of the present paper is to propose simple analytical tools for the evaluation of the transient dynamic amplifications induced by successive loads preliminary to any detailed numerical studies whenever needed. The developments are restricted to bounded elastic media, and particularly beams, and oriented toward practical engineering applications for real cases of weakly damped structures. In section 2, we introduce our basic notations and some general, well-known notions on vibrations of Euler–Bernoulli beams. These elements are used in section 3 to calculate the time response of such a beam model subjected to a succession of massless point loads and assess the dynamic magnification they can produce. These preliminary considerations allow us to derive in section 4 a simplified method for the direct calculation of the expected maximum dynamic deflection of the beam under successive loads by considering only few simple parameters related to the bridge and the train. In section 5, we give some indications on the possible modifications of the theory considering the effects of shear deformation and rotatory inertia according to Timoshenko's beam model. We finally draw some conclusions and recommendations in section 6.

2. NOTATION AND GENERAL CONSIDERATIONS

The purpose of this section is to introduce the notation used throughout this paper, as well as to recall briefly the basic notions on beam vibrations and modal analysis which shall be applied. We first consider the case of the Euler–Bernoulli beam model described by the following partial differential equation:

$$\rho \frac{\partial^2 z}{\partial t^2}(s,t) - 2\zeta \sqrt{\rho D}\, \frac{\partial}{\partial t} \frac{\partial^2 z}{\partial s^2}(s,t) + \frac{\partial^2}{\partial s^2}\left(D \frac{\partial^2 z}{\partial s^2}(s,t) \right) = x(s,t), \tag{1}$$

where z is the beam deflection due to planar bending, which depends on the position s along the beam and on time t, ρ is the mass of the beam per unit length, D is its bending rigidity,

assumed constant along the beam, ζ is the critical damping rate, and x are the externally applied loads, which depend on the position and time. In the above equation the position s belongs to the set $\Omega =]0, L[$ where L is the span length of the beam, and t is in the set $[0, +\infty[$. The initial conditions at time $t_0 = 0$ are given by the functions $f(s)$ and $g(s)$:

$$z(s, 0) = f(s); \quad \frac{\partial z}{\partial t}(s, 0) = g(s) \quad \forall s \in \bar{\Omega}. \tag{2}$$

Finally, the boundary conditions are written $\forall t \geqslant 0$

$$\begin{aligned} &z(0, t) = Z_0; \quad z(L, t) = Z_1, \\ &\frac{\partial z}{\partial s}(0, t) = \theta_0; \quad \frac{\partial z}{\partial s}(L, t) = \theta_1, \\ &-D\frac{\partial^2 z}{\partial s^2}(0, t) = \mathscr{M}_0; \quad -D\frac{\partial^2 z}{\partial s^2}(L, t) = \mathscr{M}_1, \\ &D\frac{\partial^3 z}{\partial s^3}(0, t) = T_0; \quad D\frac{\partial^3 z}{\partial s^3}(L, t) = T_1 \end{aligned} \tag{3}$$

for, respectively, the deflection, rotation (slope), moment and shear force of the beam at both supports.

The solution of this boundary value problem is projected on the eigenmodes basis, hereafter denoted by $\{\varphi_j(s)\}_{j \geqslant 1}$, as

$$z(s, t) = \sum_{j=1}^{+\infty} q_j(t)\varphi_j(s), \tag{4}$$

where $\{q_j(t)\}_{j \geqslant 1}$ are the generalized co-ordinates of the beam deflection. In the following, the eigenmodes are normalized with respect to the mass, that is, they satisfy the orthogonality condition

$$\frac{1}{L}\int_{\Omega} \varphi_j(s)\varphi_k(s)\,\mathrm{d}s = \delta_{jk}\,, \tag{5}$$

where δ is the Kronecker symbol. The associated eigenvalues are denoted by $\{\alpha_j^2\}_{j \geqslant 1}$ and correspond to the eigenfrequencies $\{\omega_j\}_{j \geqslant 1}$ such that

$$\omega_j = \frac{\alpha_j^2}{L^2}c$$

with $c^2 = D/\rho$. The generalized co-ordinates are solutions of the ordinary differential equations:

$$\begin{aligned} &\ddot{q}_j(t) + 2\zeta\omega_j\dot{q}_j(t) + \omega_j^2 q_j(t) = \frac{1}{M}\int_{\Omega} x(s, t)\varphi_j(s)\,\mathrm{d}s, \qquad t > 0 \\ &q_j(0) = \frac{1}{L}\int_{\Omega} f(s)\varphi_j(s)\,\mathrm{d}s; \;\; \dot{q}_j(0) = \frac{1}{L}\int_{\Omega} g(s)\varphi_j(s)\,\mathrm{d}s \end{aligned} \tag{6}$$

for all integers $j \geqslant 1$, $M = \rho L$ being the total mass of the beam. The generalized loads are denoted by $x_j(t) = \int_{\Omega} x(s, t)\varphi_j(s)\,\mathrm{d}s$. These equations can be generalized further by assuming a different critical damping rate ζ_j for each eigenfrequency, which is done in the rest of the paper. The damped eigenfrequencies are denoted by $\{\omega_{Dj}\}_{j \geqslant 1}$ with $\omega_{Dj} = \omega_j\sqrt{1 - \zeta_j^2}$.

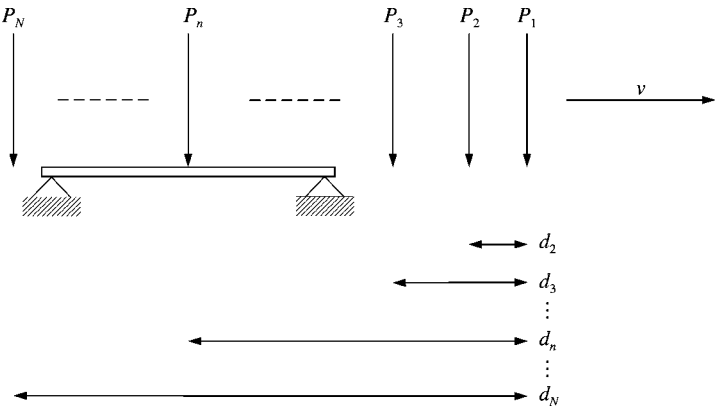

Figure 1. Layout of N successive point loads passing by a beam structure at constant speed v.

Four standard cases of boundary conditions will be considered in this study: the first one is a simply supported (hinged–hinged) beam, the second one is a clamped–clamped beam, the third one is a clamped–hinged beam, and the last one a cantilever (clamped–free) beam. The analytical expressions for the corresponding normalized eigenmodes can be found in any textbook on structural dynamics (see reference [27] for instance). Although limited to beams with a single degree of freedom for bending (the deflection), the analysis developed in this paper can be extended to vector-valued eigenmodes for multi-degree-of-freedom bounded media. Thus, provided analytical expressions are known for the eigenmodes, the developments presented below can be carried out for such structures as well (see reference [28] for the case of plates).

3. RESPONSE TO MOVING LOADS

3.1. DEFINITION OF THE MOVING LOADS

The externally applied loads consist in a succession of N concentrated point loads acting transversally on the beam and moving at a constant speed v (see Figure 1). Their weights are denoted by P_n and their relative distances with respect to the first load by d_n, for $n = 1, 2, \ldots, N$ with the convention that $d_1 = 0$. Therefore, $x(s, t)$ can be expressed by

$$x(s,t) = \sum_{n=1}^{N} P_n \mathbf{1}_{[d_n/v,(d_n+L)/v]}(t)\delta(s - vt + d_n), \tag{7}$$

where $\mathbf{1}_{\mathrm{I}}(t) = 1$ if $t \in \mathrm{I}$, $\mathbf{1}_{\mathrm{I}}(t) = 0$ if $t \notin \mathrm{I}$, and δ is the Dirac measure. Introducing the circular frequencies $\bar{\omega}_j = \alpha_j(v/L)$ corresponding to a single load travelling across the beam, the generalized loads are given by

$$x_j(t) = \sum_{n=1}^{N} P_n \mathbf{1}_{[0,L/v]}\left(t - \frac{d_n}{v}\right)\varphi_j\left(\bar{\omega}_j\left(t - \frac{d_n}{v}\right)\right). \tag{8}$$

These expressions can now be used to solve equations (6) with the principle of superposition, assuming the beam is at rest at the initial time $t_0 = 0$ when the first load P_1 reaches it, that is $f(s) = g(s) = 0$ for $s \in \bar{\Omega}$.

3.2. DYNAMIC DEFLECTION FOR A SIMPLY SUPPORTED BEAM

The beam deflection induced by each load can be decomposed into two steps: the first one corresponds to the forced vibrations due to the load P_n considered, for $d_n/v \leqslant t \leqslant (d_n + L)/v$, and the second one corresponds to the free vibrations after the load P_n has left the beam, for $t \geqslant (d_n + L)/v$. Analytical expressions can be obtained directly from equation (6) by integration; however, they are reproduced here only for the case of a simply supported beam for illustration purposes. Expressions for the other boundary conditions considered in this study may be found, for instance, in references [13, 29]. Introducing the factor $\kappa_j = \bar{\omega}_j/\omega_j$, sometimes called a speed parameter in the literature (see for instance reference [15]), the generalized co-ordinates for the deflection of a simply supported beam due to the load P_n are denoted by $q_j^{(n)}(t)$ for $j \geqslant 1$ and are given by

First step $d_n/v \leqslant t \leqslant (d_n + L)/v$:

$$q_{j1}^{(n)}(t) = \frac{\sqrt{2}P_n}{M\omega_j^2}\frac{1}{(1-\kappa_j^2)^2 + (2\zeta_j\kappa_j)^2} \times \left\{ \begin{array}{l} (1-\kappa_j^2)\sin\bar{\omega}_j\left(t - \dfrac{d_n}{v}\right) - 2\zeta_j\kappa_j\cos\bar{\omega}_j\left(t - \dfrac{d_n}{v}\right) - \kappa_j \mathrm{e}^{-\zeta_j\omega_j(t-(d_n/v))} \\ \times\left[\dfrac{(1-\kappa_j^2-2\zeta_j^2)}{\sqrt{1-\zeta_j^2}}\sin\omega_{D_j}\left(t - \dfrac{d_n}{v}\right) - 2\zeta_j\cos\omega_{D_j}\left(t - \dfrac{d_n}{v}\right)\right] \end{array} \right\}. \tag{9}$$

Note that these terms do not correspond to purely forced vibrations as they also include free vibrations induced by the impact of the loads. However, they will be called "forced vibrations" in the rest of the paper since they arise for the time intervals when the loads traverse the beam. For weakly damped structures, equation (9) can be simplified by neglecting the terms of orders greater than 1 in ζ_j. This leads to

$$q_{j1}^{(n)}(t) \simeq \frac{\sqrt{2}P_n}{M\omega_j^2}\frac{1}{1-\kappa_j^2}\left[\sin\kappa_j\omega_j\left(t - \frac{d_n}{v}\right) - \kappa_j\sin\omega_j\left(t - \frac{d_n}{v}\right)\mathrm{e}^{-\zeta_j\omega_j(t-(d_n/v))}\right] \tag{10}$$

for $\kappa_j \neq 1$, and

$$q_{j1}^{(n)}(t) \simeq \frac{-\sqrt{2}P_n}{2M\omega_j^2}\left[\omega_j\left(t - \frac{d_n}{v}\right)\cos\omega_j\left(t - \frac{d_n}{v}\right) - \sin\omega_j\left(t - \frac{d_n}{v}\right)\mathrm{e}^{-\zeta_j\omega_j(t-(d_n/v))}\right] \tag{11}$$

for $\kappa_j = 1$. The overall generalized co-ordinates for the beam forced deflection induced by the whole train of loads are

$$q_{j1}(t) = \sum_{n=1}^{N} \mathbf{1}_{[0,L/v]}\left(t - \frac{d_n}{v}\right) q_{j1}^{(n)}(t). \tag{12}$$

Second step $t \geqslant (d_n + L)/v$:

$$q_{j2}^{(n)}(t) = \frac{\sqrt{2}P_n}{M\omega_j^2}\frac{\kappa_j}{((1-\kappa_j^2)^2 + (2\zeta_j\kappa_j)^2)}\ \mathrm{e}^{-\zeta_j\omega_j(t-(d_n+L)/v)} \times\left[Q_j\cos\omega_{D_j}\left(t - \frac{d_n+L}{v}\right) + \left(\frac{\zeta_j Q_j}{\sqrt{1-\zeta_j^2}} + \frac{\dot{Q}_j}{\omega_{D_j}}\right)\sin\omega_{D_j}\left(t - \frac{d_n+L}{v}\right)\right], \tag{13}$$

where the "initial conditions" for free vibrations after the load P_n has left the beam are

$$Q_j = \mathrm{e}^{-\zeta_j j\pi/\kappa_j}\left[\frac{(1-\kappa_j^2-2\zeta_j^2)}{\sqrt{1-\zeta_j^2}}\sin\left(\frac{j\pi}{\kappa_{j'}}\right)+2\zeta_j\cos\left(\frac{j\pi}{\kappa_{j'}}\right)\right]-2(-1)^j\zeta_j$$

$$\frac{\dot{Q}_j}{\omega_j} = (-1)^j(1-\kappa_j^2)-\mathrm{e}^{-\zeta_j j\pi/\kappa_j} \times\left[\begin{array}{l}(1-\kappa_j^2-2\zeta_j^2)\left(\cos\left(\dfrac{j\pi}{\kappa_{j'}}\right)-\dfrac{\zeta_j}{\sqrt{1-\zeta_j^2}}\sin\left(\dfrac{j\pi}{\kappa_{j'}}\right)\right)\\ +2\zeta_j\left(\sqrt{1-\zeta_j^2}\sin\left(\dfrac{j\pi}{\kappa_{j'}}\right)+\zeta_j\cos\left(\dfrac{j\pi}{\kappa_{j'}}\right)\right)\end{array}\right]$$

with $\kappa_{j'} = \kappa_j/\sqrt{1-\zeta_j^2}$ and $\alpha_j = j\pi$ for a simply supported beam. For weakly damped structures, these expressions are simplified to give

$$q_{j2}^{(n)}(t) \simeq \frac{\sqrt{2}P_n}{M\omega_j^2}\frac{\kappa_j}{(1-\kappa_j^2)}\,\mathrm{e}^{-\zeta_j\omega_j(t-(d_n+L)/v)} \times\left[Q_j\cos\omega_j\left(t-\frac{d_n+L}{v}\right)+\frac{\dot{Q}_j}{\omega_j}\sin\omega_j\left(t-\frac{d_n+L}{v}\right)\right] \tag{14}$$

for $\kappa_j \neq 1$ with

$$Q_j = -\sin\left(\frac{j\pi}{\kappa_j}\right)\mathrm{e}^{-\zeta_j j\pi/\kappa_j},$$

$$\frac{\dot{Q}_j}{\omega_j} = (-1)^j-\cos\left(\frac{j\pi}{\kappa_j}\right)\mathrm{e}^{-\zeta_j j\pi/\kappa_j}.$$

The case $\kappa_j = 1$ is examined in section 4.1. Finally, the overall generalized co-ordinates for the free vibrations after the loads have left the beam one by one, are

$$q_{j2}(t) = \sum_{n=1}^{N}\mathrm{H}\left(t-\frac{d_n+L}{v}\right)q_{j2}^{(n)}(t), \tag{15}$$

where $\mathrm{H}(t)$ is the Heaviside step function, $\mathrm{H}(t) = 1$ if $t \geqslant 0$ and $\mathrm{H}(t) = 0$ if $t < 0$. To conclude this subsection, it can be noted that an alternative representation of the solution to the single load problem for an undamped simply supported beam has been given by Steele [10] in terms of an infinite series of infinite integrals. It is claimed that its convergence is improved for a high-speed parameter κ_1 as compared to the classical Fourier series representation developed here. More recently, Pesterev and Bergman [30] have derived an alternative series representation, exhibiting explicitly the quasi-static contribution to the response and converging more rapidly. The latter property can be helpful for the evaluation of spatial derivatives of the deflection, in order to calculate the distributed efforts in the beam.

3.3. DYNAMIC AMPLIFICATION FACTORS

3.3.1. *Forced vibrations of a simply supported beam*

The forced vibrations of the beam, characterized by the generalized coordinates $q_{j1}^{(n)}(t)$ for each load P_n and time $d_n/v \leqslant t \leqslant (d_n + L)/v$, are seen from equation (9) or (10) to be a combination of vibrations at the circular frequencies $\bar{\omega}_j$ for a single load traversing the beam, and ω_{Dj} for the damped eigenfrequencies of the beam. They have been extensively studied in the literature [7, 12, 25, 31, 32] and constitute the basis of the definition of the dynamic amplification factors in some standard bridge design codes, such as the Eurocode or the UIC (International Union of Railways) norms. These amplification factors are usually given as functions of κ_1 when the analysis is restricted to the fundamental eigenmode of the beam, that is when expansion (4) is truncated at $j = 1$.

We deduce from expression (9) that an apparent resonance occurs when $\kappa_j^2 = 1 - 2\zeta_j^2$, that is when $\bar{\omega}_j = \omega_j \sqrt{1 - 2\zeta_j^2}$ which is the well-known damped frequency of resonance of the single oscillator (see for instance reference [27]). The maximum deflection for the corresponding loads speed is reached when $t = (d_n + L)/jv$ and is

$$\max_{0 \leqslant t - d_n/v \leqslant L/v} q_{j1}^{(n)}(t) = \frac{\pi}{2} \times \frac{\sqrt{2} P_n}{M \omega_j^2}$$

for the undamped case. In fact, this value is only a pseudo-resonance: true resonance occurs at least for a whole period, but in this case the vibrations at the circular frequency $\bar{\omega}_j$ are defined just over an half period since $0 \leqslant t - d_n/v \leqslant L/v$. The overall maximum value of $q_{j1}^{(n)}(t)$ is rather obtained for $\kappa_j \simeq 0{\cdot}61$ and is about

$$\max_{0 \leqslant t - d_n/v \leqslant L/v} q_{j1}^{(n)}(t) \simeq 1{\cdot}73 \times \frac{\sqrt{2} P_n}{M \omega_j^2} \tag{16}$$

for a simply supported beam (see references [12, 31]). These values for each generalized co-ordinate have to be compared with the static deflection of such a beam due to a single load P at a distance ℓ from either support:

$$z_{stat}(s) = \frac{2P}{M} \sum_{j=1}^{+\infty} \frac{1}{\omega_j^2} \sin\left(j\pi \frac{\ell}{L}\right) \sin\left(j\pi \frac{s}{L}\right), \quad s \in \bar{\Omega}.$$

Furthermore, the effects of the N loads on forced vibrations do not cumulate since the action of each load is limited to time intervals of length L/v which do not overlap except for few successive loads. Indeed, for typical span lengths and trains, only 2 or 3 loads would be on the bridge at the same time; from a conservative point of view, the maximum amplifications outlined above may be multiplied by the maximum possible number of loads on the bridge, which is limited to only few of them. This means that, as regards forced vibrations, the maximum dynamic deflection can be evaluated by multiplying the maximum static deflection observed under the train layout considered, by a dynamic amplification factor $\Phi(\kappa_1)$ possibly varying with speed (as in references [12, 33]) but never greater than about 1·7 for a simply supported beam. Qualitatively, similar conclusions can be drawn for other types of boundary conditions although this last maximum amplification factor is generally slightly smaller (see for instance, the results obtained in references [13, 29]). $\Phi(\kappa_1)$ is plotted in Figure 2 for the four types of boundary conditions considered here, and according to the approximate formula proposed in reference [33] for comparison.

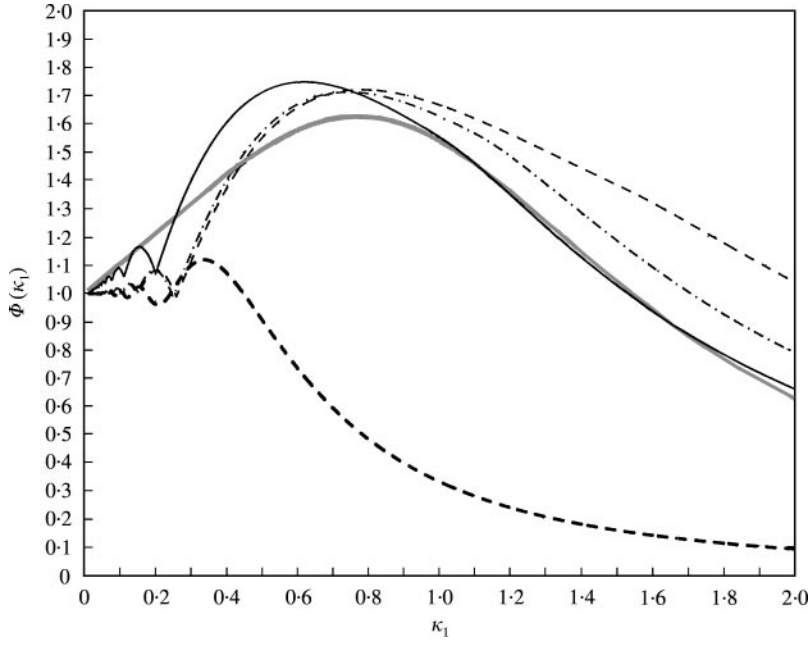

Figure 2. Dynamic amplification factor $\Phi(\kappa_1)$ as proposed in reference [33] (———) and for a simply supported beam (———), clamped–clamped beam (– – – – –), clamped–hinged beam (–·–·–·–) and cantilever beam (— — — —).

It is also worth noting at this stage that, for typical engineering structures, such as railway bridges, the span lengths are of the order of several tens of meters, and the fundamental frequency is about several Hertz. Thus, the resonance frequency for a single load travelling across the bridge corresponds to a train speed of about several hundred meters per second (or of the order of 1000 km/h), which is unrealistic for the actual vehicles.

3.3.2. *Free vibrations*

The free vibrations of the beam, characterized by the generalized co-ordinates $q_{j2}^{(n)}(t)$ for each load P_n and time $t \geqslant (d_n + L)/v$, are vibrations at the damped eigenfrequencies of the beam only. From equation (13) or (14) for weak damping, it is seen that each $q_{j2}^{(n)}(t)$ can be rewritten as

$$q_{j2}^{(n)}(t) = \frac{1}{M\omega_j^2} \frac{\kappa_j R_j(\kappa_j, \zeta_j)}{[(1-\kappa_j^2)^2 + (2\zeta_j\kappa_j)^2]}$$

$$\times P_n \sin \omega_{D_j} \left(t - \frac{d_n + L}{v} + \phi_j(\kappa_j, \zeta_j) \right) \mathrm{e}^{-\zeta_j \omega_j (t - (d_n + L)/v)}, \tag{17}$$

where

$$R_j^2 = 2\left[Q_j^2 + \frac{1}{(1-\zeta_j^2)} \left(\zeta_j Q_j + \frac{\dot{Q}_j}{\omega_j} \right)^2 \right]$$

depends on κ_j and ζ_j, and

$$\phi_j = \arctan\left(\frac{\sqrt{1-\zeta_j^2}\,Q_j}{\zeta_j Q_j + \dot{Q}_j/\omega_j}\right)$$

is an additional phase term which is independent of the current load characteristic P_n or d_n as well. Therefore, extending the above analysis to all kinds of boundary conditions considered in this study, the generalized co-ordinates of the beam free vibrations have the form

$$q_{j2}(t) = \frac{1}{M\omega_j^2}\,\frac{\kappa_j R_j(\kappa_j,\zeta_j)}{[(1-\kappa_j^2)^2 + (2\zeta_j\kappa_j)^2]} \times \sum_{n=1}^{N} P_n \mathrm{H}\left(t - \frac{d_n + L}{v}\right) \sin\omega_{Dj}\left(t - \frac{d_n + L}{v} + \phi_j(\kappa_j,\zeta_j)\right) \mathrm{e}^{-\zeta_j\omega_j(t-(d_n+L)/v)}, \tag{18}$$

where R_j depends on the type of boundary conditions. The beam free motion is thus given by the product of an amplification factor which depends on κ_j (and damping) only, and of damped free vibrations at the eigenfrequencies of the beam whose amplitudes and phases are fully characterized by the speed and layout of the moving loads. These terms are studied in detail in the next section, introducing the notions of dynamic amplification coefficient, train characteristic response spectrum and a new parameter called the loads wavelength. Note that here, contrary to the case of forced vibrations, the effects of all loads cumulate—however, with different phases—since they arise on overlapping time intervals of infinite lengths, and may thus induce non-negligible deflections as compared to the ones due to the forced vibrations for weakly damped structures. These residual free vibrations [12] for successive loads have often been disregarded in the literature.

4. ASSESSMENT OF MAXIMUM VIBRATION LEVELS

Equation (18) suggests that the leading effect of the loads on the vibrations of the beam is their frequency of succession, that is the ratio of their speed to a "typical" distance between them. In fact, it will be shown that this effect is more likely to induce resonance of the beam than the forced circular frequency $\bar{\omega}_j$ attached to a single load, for the reasons mentioned above in sections 3.3.1 and 3.3.2. For a meaningful analysis of this effect on the generalized co-ordinates for free vibrations of the beam, it is suggested that a new parameter be introduced, the so-called wavelength of the loads, defined by $\lambda = 2\pi v/\omega$. Its values at the eigenfrequencies of the beam are denoted by $\lambda_j = 2\pi v/\omega_j$. Another interesting point is to introduce the well-known simplified formula for the fundamental frequency of a beam in bending which is [12]

$$f_1 \simeq 0{\cdot}18\sqrt{\frac{g}{z_M}}, \tag{19}$$

where $g = 9{\cdot}81\ \mathrm{m/s^2}$ is the acceleration due to gravity and z_M is the beam maximum static deflection due to its own weight. Equation (19) is *a posteriori* valid for any kind of boundary conditions (the coefficient for a cantilever beam is slightly greater than 0·18 but this value is conservative as it is used hereafter). Since $\kappa_j = (\alpha_j/2\pi)\,(\lambda_j/L)$, $q_{j2}(t)$ can now be

rewritten as

$$q_{j2}(t) = z_1 \times r_j\left(2\pi\frac{L}{\lambda_j}, \zeta_j\right) \times \Sigma_j\left(t - \frac{L}{v}; \lambda_j, \zeta_j\right), \tag{20}$$

$r_j(u, \zeta)$ is a dynamic amplification coefficient defined by

$$r_j(u, \zeta) = \frac{\pi}{2} \times \frac{\alpha_1^4}{\alpha_j^4} \times \frac{u^2}{[(u^2 - \alpha_j^2)^2 + (2\zeta\alpha_j u)^2]} R_j\left(\frac{\alpha_j}{u}, \zeta\right), \tag{21}$$

$\Sigma_j(t; \lambda, \zeta)$ is a train characteristic response function associated with the free vibrations of the beam defined by

$$\Sigma_j(t; \lambda, \zeta) = \frac{1}{(0{\cdot}18\pi)^2} \times \frac{1}{\lambda} \sum_{n=1}^{N} P_n \mathrm{H}\left(\omega_j t - 2\pi\frac{d_n}{\lambda}\right) \sin\sqrt{1-\zeta^2}\left(\omega_j t - 2\pi\frac{d_n}{\lambda} + \bar{\phi}_j\right) \mathrm{e}^{-\zeta(\omega_j t - 2\pi d_n/\lambda)} \tag{22}$$

with $\bar{\phi}_j = \omega_j \phi_j$. These last two functions are studied in detail in the following subsections. Finally, z_1 is the beam maximum static deflection due to uniform distributed load of 1, that is $z_1 = z_M/\rho g$.

4.1. DYNAMIC AMPLIFICATION COEFFICIENT

The dynamic amplification coefficient r_1 defined above is plotted in Figure 3 for different values of damping and the four types of boundary conditions considered in this study. r_2 is also plotted in Figure 4 (note the difference of scales as compared to Figure 3). It is seen that, for weakly damped structures, these coefficients are almost independent of the critical damping rate ζ_j. Thus, the dependence on ζ_j will be ignored for them in the rest of the paper. They are also rapidly decreasing when j increases; thus, a truncation at the order $j = 1$ is fully justified.

Following these conclusions, we introduce a slightly different dynamic amplification coefficient denoted by $a(L/\lambda)$, independent of ζ and used hereafter to assess the maximum deflection due to free vibrations. It is defined by

$$a\left(\frac{L}{\lambda}\right) = r_1\left(2\pi\frac{L}{\lambda}, 0\right) \times \max_{s \in \bar{\Omega}} \varphi_1(s). \tag{23}$$

Figure 5 displays a for the four cases of boundary conditions considered in this paper. Its analytical expression for a simply supported beam is for instance,

$$a(u) = \left|\frac{2\cos\pi u}{1 - 4u^2}\right|$$

for $u \neq \frac{1}{2}$ and $a(\frac{1}{2}) = \pi/2$ (which is not the maximum). The formulas for other boundary conditions have been derived in reference [13]. They show that the shorter the span length is, the larger the dynamic amplification coefficients are. Furthermore, the amplification cancels out—or almost cancels out—for some particular ratios of the span length to the wavelength, whereas it has local maxima for some other ratios. In the case of a simply supported beam, these ratios are of the form $(2m - 1)/2$ and $\simeq m$ (but never exactly),

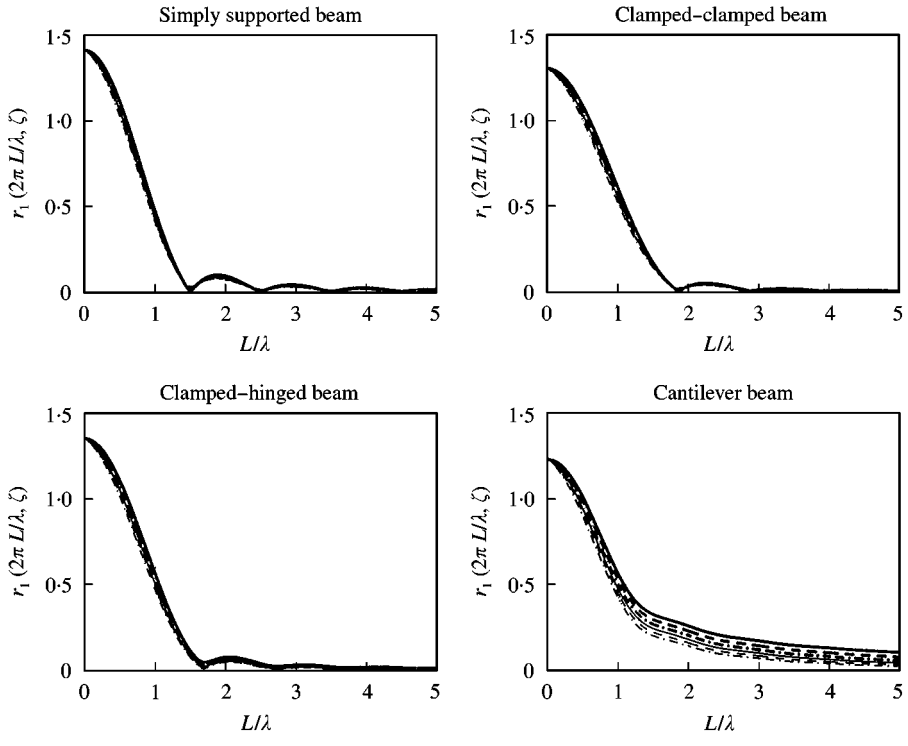

Figure 3. Dynamic amplification coefficient $r_1(2\pi L/\lambda, \zeta)$ for a simply supported beam, clamped–clamped beam, clamped–hinged beam and cantilever beam, and various damping rates ζ (———), $\zeta = 0{\cdot}5\%$; — — — —, $\zeta = 1\%$; –·–·–·–, $\zeta = 2\%$; ————, $\zeta = 3\%$; – – – – –, $\zeta = 4\%$; –·–·–·, $\zeta = 5\%$).

respectively, where $m > 1$ is an integer. For instance, for a train with a regular distance d between its successive bogies, dynamic effects on bridges are dramatically reduced by considering span lengths of order $L \simeq 1{\cdot}5\,d$. These observations are well known by railway engineers and were made in other previous analytical studies [12, 13, 15].

4.2. TRAIN RESPONSE SPECTRUM

The response spectrum of an externally applied load $x(t)$ is the maximum response with time of a single oscillator subjected to this load [27], namely,

$$\sigma(\omega, \zeta) = \frac{1}{M\omega_D} \max_{t \geqslant 0} \left| \int_0^t \sin \omega_D (t - \tau)\, \mathrm{e}^{-\zeta\omega(t-\tau)} x(\tau)\, \mathrm{d}\tau \right|,$$

where ω is the circular eigenfrequency of the oscillator, ζ is its critical damping rate and $\omega_D = \omega\sqrt{1 - \zeta^2}$. The response spectrum of the load for $\zeta = 0$ is usually close to the amplitude of its Laplace transform; however, it remains a one-to-one transform which does not permit the recovery of the load from the knowledge of its spectrum. The so-called primary response spectrum is the maximum response of the single oscillator for the duration of the loading, whereas the secondary spectrum is the maximum response after its end (damped free vibrations). Clearly, from the above analysis the secondary spectrum dominates for successive moving loads and needs to be evaluated.

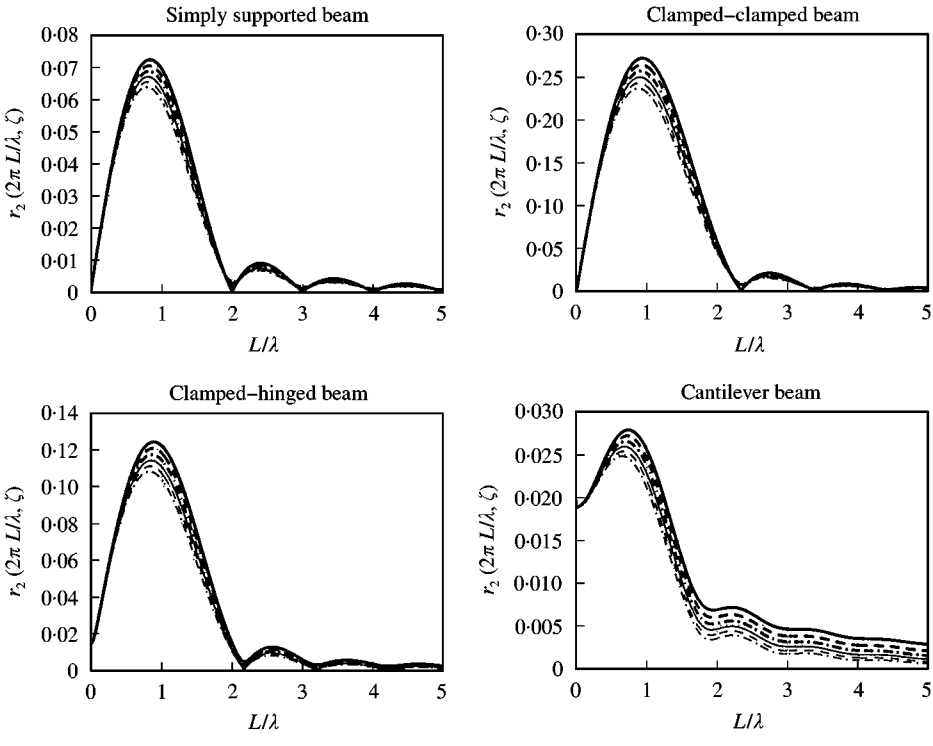

Figure 4. Dynamic amplification coefficient $r_2(2\pi L/\lambda, \zeta)$ for a simply supported beam, clamped–clamped beam, clamped–hinged beam and cantilever beam, and various damping rates ζ (———, $\zeta = 0{\cdot}5\%$; — — — —, $\zeta = 1\%$; –·–·–·–, $\zeta = 2\%$; ———, $\zeta = 3\%$; – – – – –, $\zeta = 4\%$; –·–·–·–·–, $\zeta = 5\%$).

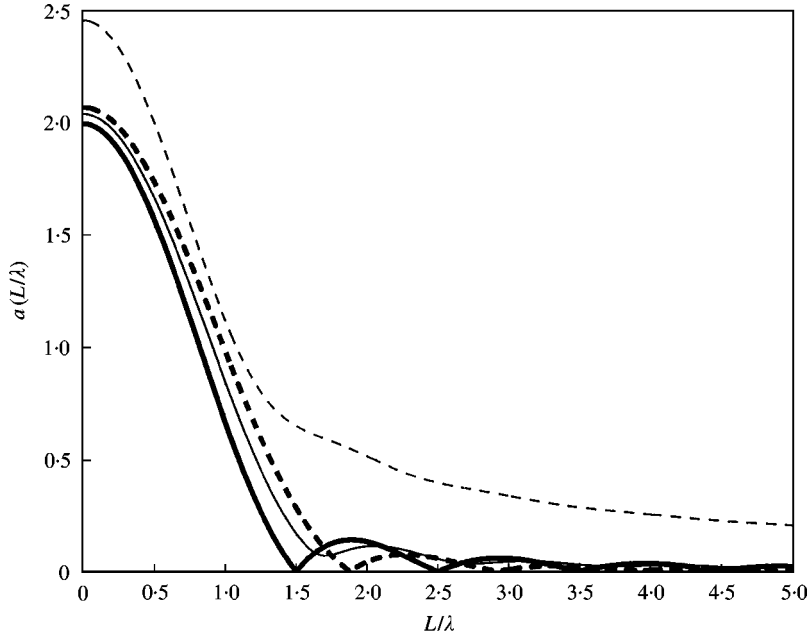

Figure 5. Dynamic amplification coefficient $a(L/\lambda)$ for a simply supported beam (———), clamped–clamped beam (— — — —), clamped–hinged beam (———) and cantilever beam (– – – – –).

Here we define the secondary train response spectrum as the maximum of $\Sigma_j(t;\lambda,\zeta)$ with time and the number of loads, to account for the difference in phase between them

$$\sigma_j(\lambda,\zeta) = \max_{1\leqslant N_s\leqslant N}\ \max_{t\geqslant 0} \frac{1}{(0{\cdot}18\pi)^2}\frac{1}{\lambda}\left|\sum_{n=1}^{N_s} P_n \mathrm{H}\left(\omega_j t - 2\pi\frac{d_n}{\lambda}\right)\right.$$
$$\left.\times \sin\sqrt{1-\zeta^2}\left(\omega_j t - 2\pi\frac{d_n}{\lambda} + \bar{\phi}_j\right)\mathrm{e}^{-\zeta(\omega_j t - 2\pi d_n/\lambda)}\right|. \tag{24}$$

This series is still quite cumbersome and (very) costly to evaluate numerically. However, the response spectrum as it is defined above is well approximated by $\sigma(\lambda,\zeta)$ where

$$\sigma(\lambda,\zeta) = \frac{1}{(0{\cdot}18\pi)^2}\max_{1\leqslant N_s\leqslant N}\frac{1}{\lambda}\left|\sum_{n=1}^{N_s} P_n \exp\left[2\pi\left(-\zeta + \mathrm{i}\sqrt{1-\zeta^2}\right)\frac{d_n}{\lambda}\right]\right| \tag{25}$$

with $\mathrm{i} = \sqrt{-1}$. The series in the above expression is nothing but the Laplace transform of the generalized loads $x_j(t)$ evaluated at the poles $p_j = -\zeta_j\omega_j + \mathrm{i}\omega_{Dj}$ of sub-critically damped single oscillators with circular eigenfrequencies ω_j and critical damping rates ζ_j. This formula has the advantage of being independent from the geometrical and mechanical characteristics of the beam, apart from its critical damping ratio, although it is a relevant estimation of its true response spectrum. That is why from now on we will choose it to define the train characteristic response spectrum $\sigma(\lambda,\zeta)$ used to assess the maximum deflection of the beam under moving loads. Figure 6 displays this response spectrum for the example of a French TGV-A train whose layout is given in reference [25]. A "typical" distance between the loads is $d \simeq 19$ m (to be compared with the constant length of the cars $d = 18{\cdot}7$ m which is different from the length of the power cars) and maximum amplifications are observed for $\lambda = d$ and $d/2$. This observation can be generalized to other actual train layouts. The corresponding loads speeds are $v = d\times f_1$ and $(d/2)\times f_1$, where f_1 is the fundamental eigenfrequency of the beam, and are often called "critical" speeds. However, the beam response at these speeds remains always bounded, whereas true critical speeds would rather correspond to the limits of instability for the steady state response of infinite or semi-infinite systems (see for instance references [10, 16, 17, 23]). In agreement with Adams [14], we note that they can be much smaller than the speed corresponding to $\kappa_1 = 1$ for which we have $v = 2L\times f_1$.

To get further insight on the response spectrum, let us consider the case where $d_n = (n-1)d$ and $P_n = P$ (d and P are constant), that is a succession of regularly spaced and identical loads, and $\zeta = 0$. Then when $\lambda = d/m$, where m is a positive integer, the train spectrum is $\sigma = (1/(0{\cdot}18\pi)^2)\,(mNP/d)$. Thus, it is linear with respect to the number of loads and maximum for a frequency of succession of these loads which matches the fundamental frequency of the bridge or its fractions; of course, this linear dependence for $\zeta = 0$ is increasingly damped out when ζ increases. The critical speeds are in this case $v_m = (d/m)\times f_1$, and theoretically identical results hold for all eigenfrequencies of the beam. If $\lambda = 2d$ then the response spectrum is simply proportional to a single load $\sigma = (1/(0{\cdot}18\pi)^2)\,(P/2d)$. These observations are confirmed by Figure 7 where the response spectrum for the train used by Yang *et al.* [15] and having a more regular arrangement of loads has been displayed. Its characteristics are as follows: $d_{2n} = nd + (n-1)e$ and $d_{2n+1} = n(d+e)$, with $N = 10$ (corresponding to 5 cars), $d = 18$ m, $e = 6$ m, and $P_n = 22\times 10^3$ kg.

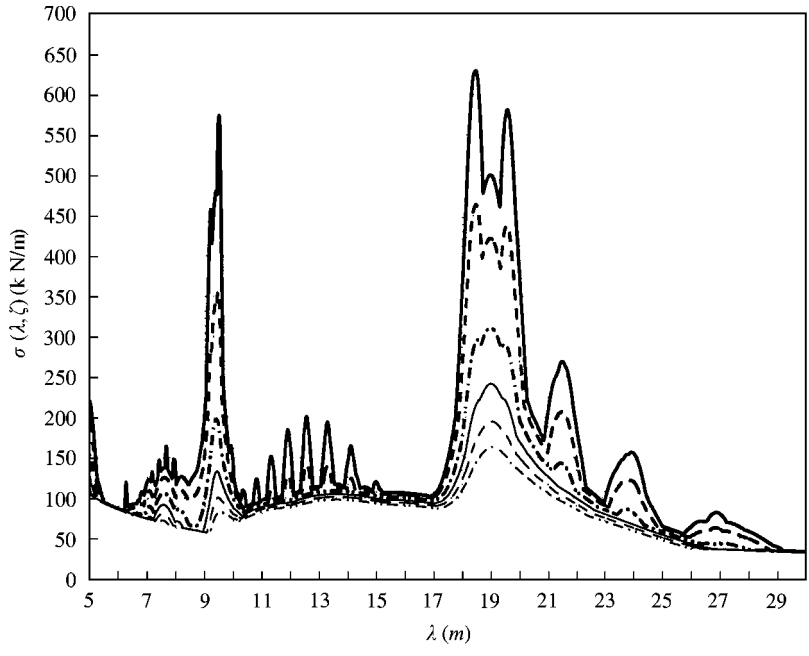

Figure 6. TGV-A characteristic response spectrum $\sigma(\lambda, \zeta)$ for various critical damping rates of the beam (———, $\zeta = 0{\cdot}5\%$; — — — —, $\zeta = 1\%$; **–·–·–·–**, $\zeta = 2\%$; ———, $\zeta = 3\%$; – – – – –, $\zeta = 4\%$; – · – · – · – · , $\zeta = 5\%$).

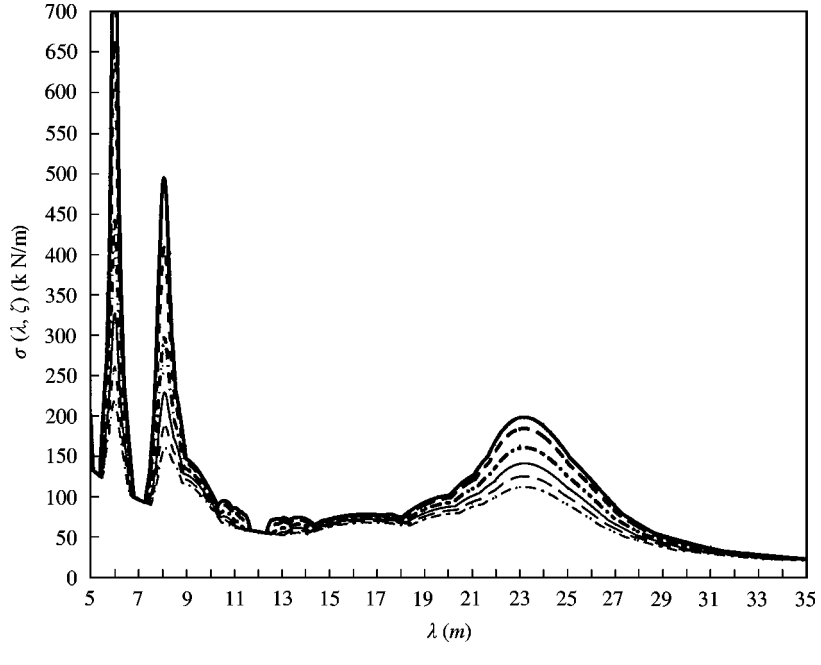

Figure 7. Response spectrum $\sigma(\lambda, \zeta)$ for the train considered by Yang *et al.* [15] and various critical damping rates of the beam (———, $\zeta = 0{\cdot}5\%$; — — — — — —, $\zeta = 1\%$; **–·–·–·–**, $\zeta = 2\%$; ———, $\zeta = 3\%$; – – – – –, $\zeta = 4\%$; – · – · – · – , $\zeta = 5\%$).

4.3. SIMPLIFIED CALCULATION OF THE MAXIMUM RESPONSE OF THE BEAM

4.3.1. *Proposed formulas*

From the previous considerations and putting together equation (4) up to the first order and equation (20), the maximum dynamic deflection of a beam under successive moving loads is

$$z_{max} \simeq \Phi\left(\frac{L}{\lambda_1}\right) \times z_{stat} + a\left(\frac{L}{\lambda_1}\right) \times \sigma(\lambda_1, \zeta) \times z_1, \tag{26}$$

where z_{stat} is the maximum static deflection of the beam under the arrangement of loads considered, z_1 is its maximum static deflection under a uniform unit load, L is the span length, ζ is the critical damping rate, λ_1 is the wavelength of the loads defined as the ratio of their speed to the fundamental frequency of the beam; finally, $\Phi \leqslant 1{\cdot}7$ is the dynamic amplification factor for the forced vibrations defined in the usual design codes and such that

$$\lim_{\lambda \to 0} \Phi\left(\frac{L}{\lambda}\right) = 1.$$

The maximum vertical acceleration of the beam can be evaluated from the above using the pseudo-acceleration spectrum associated with a given train characteristic response spectrum $\sigma(\lambda, \zeta)$:

$$\gamma_{max} \simeq a\left(\frac{L}{\lambda_1}\right) \times \omega_1^2 \sigma(\lambda_1, \zeta) \times z_1. \tag{27}$$

Note that from the formulas defining $a(L/\lambda)$ and $\sigma(\lambda, \zeta)$, it can be seen that

$$\lim_{\lambda \to 0} a\left(\frac{L}{\lambda}\right) \sigma(\lambda, \zeta) = 0$$

as expected: dynamic amplification vanishes when the train speed is zero.

Other quantities of interest for engineering applications, such as the ones mentioned in the introduction, can be derived by the same procedure using essentially equation (4). Note, however, that in doing so, it must be kept in mind that the convergence of the series deteriorates by successive spatial derivatives and then higher order terms shall be added. For instance, estimates of the maximum rotations at the hinged supports may be obtained from the above equations scaled by the span length L with a modified accordingly (maximum of $\varphi_1'(s)$ for $s = 0$ or L instead of the maximum of $\varphi_1(s)$). Besides, torsional motions are described by similar differential equations and mode shapes (depending on the boundary conditions) while the loads are multiplied by their excentricity with respect to the torsion centre of the beam.

4.3.2. *Numerical example*

We consider the case of a simply supported beam whose characteristics are chosen in accordance with the example examined by Yang *et al.* [15], and focus on the time history of the deflection at mid-span for different speeds of the loads. The plots are obtained using the exact analytical formulas given in section 3.2 and the summation of five eigenmodes. The span length is $L = 20\,\text{m}$, its density is $\rho = 34{\cdot}088\,\text{kg/m}$ and its bending rigidity is $D = 1{\cdot}12 \times 10^{11}\,\text{N m}^2$, such that its fundamental eigenfrequency is $f_1 = 7{\cdot}1\,\text{Hz}$. The static deflection under a uniform unit load of 100 kN/m is $z_1 \simeq 1{\cdot}9\,\text{mm}$. The critical damping rate is chosen as $\zeta = 2{\cdot}5\%$. The loading train is the one described in section 4.2 whose spectrum

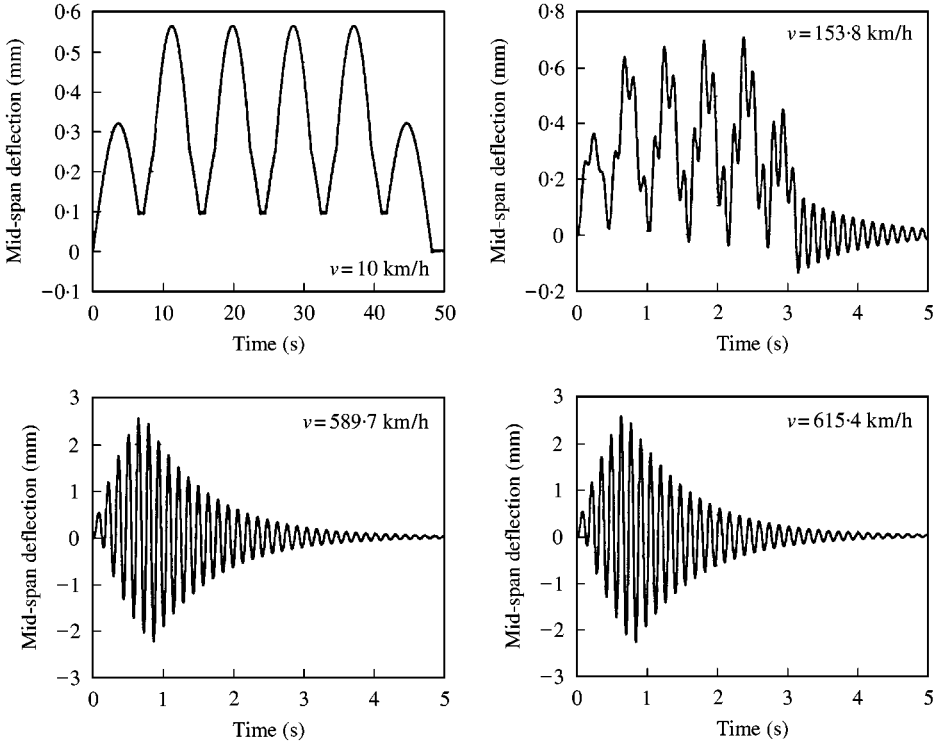

Figure 8. Time history of the deflection at mid-span of a simply supported beam at various critical speeds of the train. Train and beam characteristics are taken from reference [15].

is given in Figure 7. From the examination of this spectrum, it is seen that possible maximum amplifications can occur at $\lambda_1 \simeq 23$, 8 and 6 m corresponding to train speeds $v = 589{\cdot}7$, $205{\cdot}1$ and $v = 153{\cdot}8$ km/h respectively. Time history curves of the mid-span deflection for $v = 153{\cdot}8$ and $589{\cdot}7$ km/h are plotted in Figure 8, together with the curves for $v = 615{\cdot}5$ km/h, corresponding to $\kappa_1 = 0{\cdot}6$, and $v = 10$ km/h, corresponding to the so-called crawling (quasi-static) deflection. On the other hand, Figure 5 gives the values $L/\lambda_1 = m - \frac{1}{2}$ where dynamic amplifications can theoretically be cancelled. They correspond to the cancellation speeds $v = 341{\cdot}9$ km/h for $m = 2$, $v = 205{\cdot}1$ km/h for $m = 3$ (which is a critical speed as well), $v = 146{\cdot}5$ km/h for $m = 4$ and $v = 114$ km/h for $m = 5$. Figure 9 displays the time history deflection at mid-span for these four speeds. It is seen that dynamic amplifications are effectively cancelled out since the maximum deflections observed are comparable to the maximum crawling deflection plotted in Figure 8. For instance, if $m = 2$ then $\kappa_1 = \frac{1}{3}$ and $\Phi \simeq 1{\cdot}45$ whereas the observed amplification is $z_{max} \simeq 1{\cdot}3 \times z_{stat}$. Regarding the critical speeds, for instance, $v = 589{\cdot}7$ km/h, we have $\Phi \simeq 1{\cdot}7$, whereas $a \simeq 0{\cdot}9$ and $\sigma \simeq 140$ kN/m. Thus, $z_{max} \simeq 3{\cdot}2$ mm from equation (26), compared to $z_{max} \simeq 2{\cdot}7$ mm from Figure 8. We also observe that at $v = 153{\cdot}8$ km/h, the dynamic amplification coefficient a is negligible and $\Phi \simeq 1{\cdot}15$, so that dynamic amplifications are significantly reduced.

4.3.3. *Comparison with experiments*

The proposed formula for the expected maximum acceleration is compared with measured accelerations on an existing railway bridge in France (data provided by the

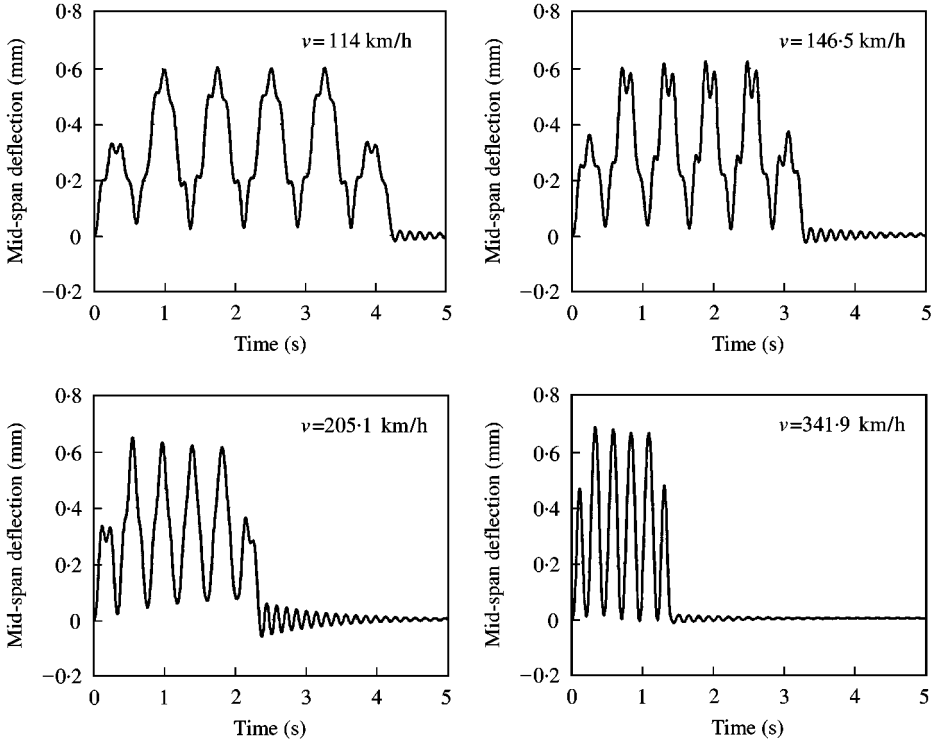

Figure 9. Time history of the deflection at mid-span of a simply supported beam at various cancellation speeds of the train. Train and beam characteristics are taken from reference [15].

French National Railways, SNCF). This simply supported structure is labelled OA71·18 and its useful characteristics are as follows: its span length is $L = 17{\cdot}4$ m, its fundamental eigenfrequency is $f_1 = 4{\cdot}5$ Hz, its critical damping rate is estimated at $\zeta_1 = 4\%$, and its mass per unit length is $\rho = 16{\cdot}3 \times 10^3$ kg/m. The bridge was traversed by a TGV-A type high-speed train at the speed $v = 260$ km/h and the maximum acceleration experienced at mid-span was $\gamma_{exp} = 3{\cdot}5$ m/s^2.

For these data, the loading wavelength λ_1 is $\lambda_1 = 16$ m leading to $a \simeq 0{\cdot}5$ for the dynamic amplification coefficient and $\sigma_{TGV} \simeq 95$ kN/m for the train spectrum. Applying equation (27), the expected maximum acceleration is found to be $\gamma_{max} \simeq 3{\cdot}8$ m/s^2 which compares reasonably well with measurements.

We conclude from these examples that the proposed formulas for the assessment of maximum vibration levels give accurate results, although slightly conservative with respect to the numerical simulations based on the exact analytical expressions, and the measured acceleration for the particular experiment described previously. The discrepancies can easily be explained by invoking the simplifying assumptions introduced as and when required for the derivation of equation (26).

5. INFLUENCE OF SHEAR DEFORMATION AND ROTATORY INERTIA

In this section, we briefly review the influence of transverse shear deformation and rotatory inertia on the results obtained so far, using the more exact Timoshenko beam

model. The developments below are intended to give some indication on how the formulas of section 4.3 may be tentatively modified or not in accordance with this alternative model.

Euler–Bernoulli beam models are valid only if the slenderness ratio r/L is small, where r is the radius of gyration. These models are also often inaccurate for beams with a constant cross-section S and mass per unit length ρ. A Timoshenko beam theory taking into account shear deformations and rotatory inertia is more adapted to such cases and when the slenderness ratio is not too small. Introducing the bending angle $\theta(s, t)$ along the beam, the basic coupled partial differential equations considered for θ and z are

$$\begin{aligned} x(s,t) - \rho \frac{\partial^2 z}{\partial t^2}(s,t) &= \frac{\partial}{\partial s}\left[k'GS\left(\theta(s,t) - \frac{\partial z}{\partial s}(s,t)\right)\right] - 2\zeta\sqrt{\rho D}\,\frac{\partial}{\partial t}\frac{\partial^2 z}{\partial s^2}(s,t), \\ \frac{\rho I}{S}\frac{\partial^2 \theta}{\partial t^2}(s,t) &= k'GS\left(\frac{\partial z}{\partial s}(s,t) - \theta(s,t)\right) + D\frac{\partial^2 \theta}{\partial s^2}(s,t), \end{aligned} \tag{28}$$

where ρ is the mass per unit length of the beam, S is its cross-section area and I is its bending inertia, $D = EI$ is the bending rigidity and E is Young's modulus; $G = E/2(1 + \nu)$ is the shear modulus, ν the Poisson coefficient, and k' is the usual shear reduction coefficient depending on ν and the cross-section geometry. The same boundary conditions and initial conditions as in section 2 are applied. We also consider that the beam is at rest at $t = 0$ ($f(s) = g(s) = 0$ for $s \in \bar{\Omega}$).

The conservative spectral problem for the beam deflection is given by the equation

$$\frac{\mathrm{d}^4\varphi}{\mathrm{d}s^4}(s) + \omega^2\left(\frac{1}{c_p^2} + \frac{1}{c_s^2}\right)\frac{\mathrm{d}^2\varphi}{\mathrm{d}s^2}(s) - \frac{\omega^2}{c^2}\left(1 - \frac{\omega^2 c^2}{c_p^2 c_s^2}\right)\varphi(s) = 0, \quad s \in \Omega \tag{29}$$

and boundary condition (3), with the following parameters:

$$c^2 = \frac{D}{\rho}, \quad r^2 = \frac{I}{S}, \quad c_p^2 = \frac{ES}{\rho} = \frac{c^2}{r^2}, \quad c_s^2 = \frac{k'GS}{\rho}.$$

The eigenmodes have expressions of the form

$$\varphi_j(s) = \sin\left(\alpha_j^+ \frac{s}{L}\right) + A_j \sinh\left(\alpha_j^- \frac{s}{L}\right) + B_j \cos\left(\alpha_j^+ \frac{s}{L}\right) + C_j \cosh\left(\alpha_j^- \frac{s}{L}\right) \tag{30}$$

up to a normalization coefficient, and the eigenvalues are given by

$$\left(\frac{\alpha_j^\pm}{L}\right)^2 = \frac{\omega_j^{\pm 2}}{2}\left[\pm\left(\frac{1}{c_p^2} + \frac{1}{c_s^2}\right) + \sqrt{\left(\frac{1}{c_p^2} - \frac{1}{c_s^2}\right)^2 + \frac{4}{\omega_j^{\pm 2} c^2}}\right] \tag{31}$$

provided that $\omega_j^\pm < c_s/r = \omega_c$.

The forced deflection of a simply supported Timoshenko beam excited by a single moving load is studied for instance in reference [34]. In this case, $\alpha_j = j\pi$ and the two sets of circular eigenfrequencies are

$$\omega_j^{\pm 2} = \gamma_j^{\pm 2}\omega_j^2 = \frac{\omega_j^2}{2\psi_j^2}\left[1 + \frac{c_s^2}{c_p^2}\left(1 + \frac{1}{\psi_j^2}\right) \pm \sqrt{\left[1 + \frac{c_s^2}{c_p^2}\left(1 + \frac{1}{\psi_j^2}\right)\right]^2 - \frac{4c_s^2}{c_p^2}}\right] \tag{32}$$

with $\psi_j = \alpha_j r/L$ (Rayleigh's coefficient). $\{\omega_j\}_{j \geqslant 1}$ are the circular eigenfrequencies for the Euler–Bernoulli beam model, which is recovered when $\omega_c \to +\infty$, so that $\omega_j^\pm \to \omega_j$. The normalized eigenmodes for the beam deflection $\{\varphi_j(s)\}_{j \geqslant 1}$ and bending angle $\{\chi_j(s)\}_{j \geqslant 1}$

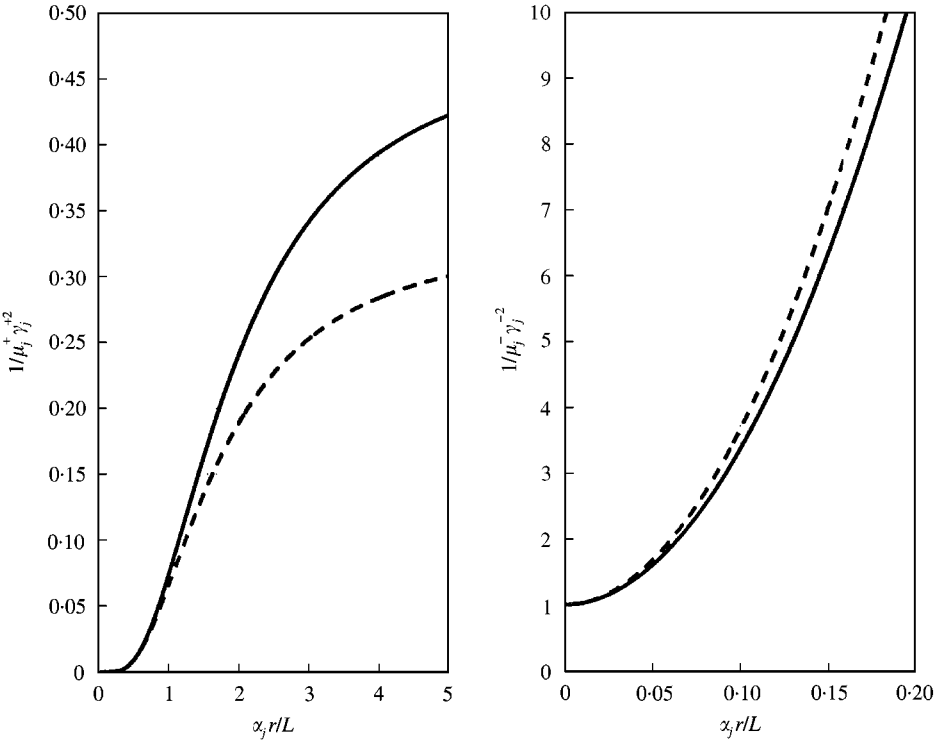

Figure 10. Coefficients $1/\mu_j^{\pm}\gamma_j^{\pm 2}$ for a circular (— — —) and a rectangular (———) Timoshenko beam with $\nu = 0{\cdot}2$.

are given by

$$\varphi_j(s) = \sqrt{\frac{2}{\mu_j^{\pm}}}\sin\left(\alpha_j \frac{s}{L}\right),$$
$$\chi_j(s) = \sqrt{\frac{2}{\mu_j^{\pm}}}\left(1 - \frac{c_p^2}{c_s^2}\gamma_j^{\pm 2}\psi_j^2\right)\frac{\alpha_j}{L}\cos\left(\alpha_j \frac{s}{L}\right), \tag{33}$$

where $\mu_j^{\pm} = 1 + \psi_j^2(1 - (c_p^2/c_s^2)\gamma_j^{\pm 2}\psi_j^2)^2$; they satisfy the orthogonality condition

$$\frac{1}{L}\int_{\Omega}\varphi_j(s)\varphi_k(s)\,\mathrm{d}s + \frac{r^2}{L}\int_{\Omega}\chi_j(s)\chi_k(s)\,\mathrm{d}s = \delta_{jk}.$$

Then it can be shown that the generalized co-ordinates satisfy the ordinary differential equations:

$$\ddot{q}_j(t) + 2\zeta_j^{\pm}\omega_j^{\pm}\dot{q}_j(t) + \omega_j^{\pm 2}q_j(t) = \frac{x_j(t)}{M\mu_j^{\pm}}, \qquad t > 0,$$
$$q_j(0) = 0, \quad \dot{q}_j(0) = 0 \tag{34}$$

with $\zeta_j^{\pm} = \zeta_j/\mu_j^{\pm}\gamma_j^{\pm}$. Therefore, all the results obtained so far are formally unchanged and the maximum response of the beam can be evaluated using equation (26) for the same

structure modellized by an Euler–Bernoulli beam, corrected by a factor $1/\mu_1^- \gamma_1^{-2} \geqslant 1$ (for the lowest eigenfrequency):

$$z_{max} \simeq \frac{1}{\mu_1^- \gamma_1^{-2}} \left[\Phi\left(\frac{L}{\lambda_1}\right) \times z_{stat} + a\left(\frac{L}{\lambda_1}\right) \times \sigma(\lambda_1, \zeta) \times z_1 \right]. \tag{35}$$

In Figure 10, we have plotted the coefficients $1/\mu_j^{\pm} \gamma_j^{\pm 2}$ as functions of ψ_j for a Poisson coefficient $v = 0{\cdot}2$ and circular and rectangular cross-sections, for which [35]

$$k' = \frac{6(1+v)}{7+6v}, \quad \text{circular cross-section,}$$

$$k' = \frac{10(1+v)}{12+11v}, \quad \text{rectangular cross-section.}$$

Similar analyses can be performed for the influence of an axial load or elastic foundation, and comparable conclusions are reached.

6. CONCLUSIONS

In this paper, the exact analytical solution for an Euler–Bernoulli beam traversed by a succession of massless point loads has been given. The dynamic amplifications corresponding to the forced response and free vibrations were both analyzed in detail. In particular, free vibrations were shown to be generally non-negligible as compared to the forced ones, if the number of loads is of the order of several tens as is the case in railway applications. Based on these results, simple formulas involving a minimum of soundly parameters were derived for the calculation of the maximum expected dynamic amplifications induced by the loads. They show that for some particular span lengths related to the wavelength of the loads, these effects can be dramatically reduced and even theoretically cancelled. Therefore, they may be especially useful in the context of preliminary design of railway structures modelled by beams. Finally, tentative formulas were also given to account for transverse shear deformations and rotatory inertia according to the Timoshenko beam model.

The simplified formulas for beams obtained in this work cannot be applied directly to some particular structures such as skewed or cable-stayed bridges for instance. In these latter cases, three-dimensional models are needed and can only be solved numerically. However, the results obtained so far could easily be extended, in our opinion, to plates since analytical expressions of the eigenmodes are available for most cases of boundary conditions and geometrical layout used in practical applications. We also note that in the evaluation of the dynamic amplification effects, structural strength may be less a concern for railway bridges than riding comfort and safety standards for the tracks in operational conditions. The formulas given in this paper are adapted to the evaluation of the maximum deformations related to the criteria applicable for accelerations in the train cars or alignment of the tracks.

ACKNOWLEDGMENTS

This study was carried out while the author was affiliated to the Systra Group, mostly in 1994. The author thanks V. T. Doan and D. Mion of the Engineering Direction at SNCF for some valuable discussions and useful suggestions.

REFERENCES

1. M. KLASZTORNY and J. LANGER 1990 *Earthquake Engineering and Structural Dynamics* **19**, 1107–1124. Dynamic response of single-span beam bridges to a series of moving loads.
2. Y.-H. LIN and M. W. TRETHEWEY 1990 *Journal of Sound and Vibration* **136**, 323–342. Finite element analysis of elastic beams subjected to moving dynamic loads.
3. H. M. METWALLY, F. K. SALMAN and A. M. EL LAKANY 1993 in *Proceedings of the* 11*th International Modal Analysis Conference*, 1564–1571. An improved matrix method for the dynamic response for modeling structure under moving vehicles. Bethel: Society for Experimental Mechanics, Inc.
4. K. HENCHI, M. FAFARD, G. DHATT and M. TALBOT 1997 *Journal of Sound and Vibration* **199**, 33–50. Dynamic behaviour of multi-span beams under moving loads.
5. R. MORENO DELGADO and S. M. DOS SANTOS 1997 *Computers and Structures* **63**, 511–523. Modelling of railway bridge–vehicle interaction on high speed tracks.
6. Y.-H. CHEN and C.-Y. LI 2000 *American Society of Civil Engineers, Journal of Bridge Engineering* **5**, 124–130. Dynamic response of elevated high-speed railway.
7. S. TIMOSHENKO, D. H. YOUNG and W. WEAVER 1974 *Vibration Problems in Engineering*. New York: John Wiley and Sons; fourth edition.
8. C. E. INGLIS 1934 *A Mathematical Treatise on Vibrations in Railway Bridges*. Cambridge: Cambridge University Press.
9. R. S. AYRE, G. FORD and L. S. JACOBSEN 1950 *Transactions of the American Society of Mechanical Engineers, Journal of Applied Mechanics* **17**, 1–12. Transverse vibration of a two-span beam under action of a moving constant force.
10. C. R. STEELE 1967 *Transactions of the American Society of Mechanical Engineers, Journal of Applied Mechanics* **34**, 111–118. The finite beam with a moving load.
11. L. FRYBA 1972 *Vibration of Solids and Structures under Moving Loads*. Groningen: Noordhoff International Publishing.
12. F. MANCEL 1992 *Dynamics of a Simply Supported Span*. Unpublished technical notes SNCF. (In French).
13. E. SAVIN 1994 *DEA Thesis dissertation, Ecole Centrale de Paris*. Dynamics of railway bridges under moving loads. (In French).
14. G. G. ADAMS 1995 *International Journal of Mechanical Sciences* **37**, 773–781. Critical speeds and the response of a tensional beam on an elastic foundation to repetitive moving loads.
15. Y.-B. YANG, J.-D. YAU and L.-C. HSU 1997 *Engineering Structures* **19**, 936–944. Vibration of simple beams due to trains moving at high speeds.
16. R. G. PAYTON 1964 *Quarterly of Applied Mathematics* **21**, 299–313. An application of the dynamic Betti–Rayleigh reciprocal theorem to moving-point loads in elastic media.
17. H. A. DIETERMAN and A. METRIKINE 1996 *European Journal of Mechanics A/Solids* **15**, 67–90. The equivalent stiffness of a half-space interacting with a beam. Critical velocities of a moving load along the beam.
18. H. S. ZIBDEH and R. RACKWITZ 1996 *Journal of Sound and Vibration* **195**, 85–102. Moving loads on beams with general boundary conditions.
19. P. SNIADY, S. BIERNAT, R. SIENIAWSKA and S. ZUKOWSKI 1999 in *Proceedings of the Third International Conference on Computational Stochastic Mechanics* (P. D. Spanos, editor), 485–490. Vibrations of the beam due to a load moving with stochastic velocity. Rotterdam: Balkema.
20. D. MINKOUSSÉ and J. COUVERT 1972 *M.Sc. Thesis dissertation, Ecole Nationale des Ponts et Chaussées*. A study of dynamic amplification phenomena for railway bridges. (In French).
21. J. PALAMAS, O. COUSSY and A. BAMBERGER 1985 *Journal of Sound and Vibration* **99**, 235–245. Effects of surface irregularities upon the dynamic response of bridges under suspended moving loads.
22. T.-L. WANG and D. HUANG 1992 *American Society of Civil Engineering, Journal of Structural Engineering* **118**, 1354–1374. Cable-stayed bridge vibration due to road surface roughness.
23. L. FRYBA, S. NAKAGIRI and N. YOSHIKAWA 1993 *Journal of Sound and Vibration* **163**, 31–45. Stochastic finite elements for a random foundation with uncertain damping under a moving force.
24. E. CHAMBRON 1976 *Revue Générale des Chemins de Fer* **95**, 717–732. Les ouvrages d'art de la ligne nouvelle.
25. P. RAMONDENC 1993 *Bulletin Ponts Métalliques* **16**, 7–23. TGV et ponts métalliques.
26. L. FRYBA 1996 *Dynamics of Railway Bridges*. London: Thomas Telford.
27. R. W. CLOUGH and J. PENZIEN 1993 *Dynamics of Structures*. New York: McGraw-Hill; second edition.

28. A. W. LEISSA 1993 *Vibrations of Plates*. Woodbury: Publications in Acoustics, Acoustical Society of America (originally published in 1969, NASA SP-160).
29. M. ABU HILAL and H. S. ZIBDEH 2000 *Journal of Sound and Vibration* **229**, 377–388. Vibration analysis of beams with general boundary conditions traversed by a moving force.
30. A. V. PESTEREV and L. A. BERGMAN 2000 *Transactions of the American Society of Mechanical Engineers, Journal of Vibration and Acoustics* **122**, 54–61. An improved series expansion of the solution to the moving oscillator problem.
31. E. S. EICHMANN 1953 *Transactions of the American Society of Mechanical Engineers, Journal of Applied Mechanics* **20**, 562. Note on the maximum effect of a moving force on a simple beam.
32. A. MATSUURA 1976 *Proceedings of the JSCE* **256**, 35–47. A study of dynamic behavior of bridge girder for high speed railway.
33. UIC 1976 *Bridges for High and Very High Speeds*. Leaflet no. 776-2; first edition. Available at http://www.uic.asso.fr/.
34. S. MACKERTICH 1990 *Journal of the Acoustical Society of America* **88**, 1175–1178. Moving load on a Timoshenko beam.
35. G. R. COWPER 1966 *Transactions of the American Society of Mechanical Engineers, Journal of Applied Mechanics* **33**, 335–340. The shear coefficient in Timoshenko's beam theory.